# Nonadiabatic Topological Energy Pumps with Quasiperiodic Driving

David M. Long,[1,*] Philip J. D. Crowley,[1,2] and Anushya Chandran[1]
[1]*Department of Physics, Boston University, Boston, Massachusetts 02215, USA*
[2]*Department of Physics, Massachusetts Institute of Technology, Cambridge, Massachusetts 02139, USA*

(Received 13 October 2020; accepted 12 February 2021; published 11 March 2021)

We derive a topological classification of the steady states of $d$-dimensional lattice models driven by $D$ incommensurate tones. Mapping to a unifying $(d+D)$-dimensional localized model in frequency space reveals anomalous localized topological phases (ALTPs) with no static analog. While the formal classification is determined by $d+D$, the observable signatures of each ALTP depend on the spatial dimension $d$. For each $d$, with $d+D=3$, we identify a quantized circulating current and corresponding topological edge states. The edge states for a driven wire ($d=1$) function as a quantized, nonadiabatic energy pump between the drives. We design concrete models of quasiperiodically driven qubits and wires that achieve ALTPs of several topological classes. Our results provide a route to experimentally access higher dimensional ALTPs in driven low-dimensional systems.

DOI: 10.1103/PhysRevLett.126.106805

*Introduction.*—Topological order in static systems can underlie the quantization of nonequilibrium responses in slowly driven systems with fewer dimensions. A well-known example is the Thouless charge pump, a slowly and periodically driven insulating wire that transmits charge at a quantized rate [1–6]. Fourier transform of the drive produces a static frequency lattice with one spatial and one synthetic dimension in the presence of a weak electric field. Charge pumping in the wire can then be understood via the integer quantum Hall effect in the frequency lattice. Analogous arguments also relate a qubit slowly driven by two incommensurate tones to a frequency lattice with two synthetic dimensions [7–12]. In this setting, the integer quantum Hall effect manifests as a quantized energy current between the two drives.

Can nonequilibrium responses be quantized away from the adiabatic limit? An affirmative answer with periodic driving is provided by the two-dimensional anomalous Floquet-Anderson insulator (AFAI), which transports charge along the boundary of the sample at a quantized rate. Charge pumping in the AFAI can be understood through a topological invariant of a frequency lattice, now with two spatial and one synthetic dimension [13,14].

In this Letter, we use the frequency lattice construction to reveal nonadiabatic topological responses in quasiperiodically driven systems. Our key observation is that the frequency lattice treats spatial and synthetic dimensions on an equal footing when its eigenstates are localized (Fig. 1). More formally, the topological classification of localized phases of $d$-dimensional tight-binding models driven by $D$ incommensurate periodic tones depends only on the total frequency lattice dimension $d+D$. The classification is by an integer when $d+D>1$ is odd and is trivial otherwise. We call the nontrivial phases anomalous localized topological phases (ALTPs).

We obtain the observable signatures of ALTPs for each $d$, with $d+D=3$ from the frequency lattice as summarized in Fig. 1. In particular, edge states in the frequency lattice manifest as a quantized energy current between the two drives for the $d=1$ wire. We verify our predictions numerically in concrete models and close with experimental implications.

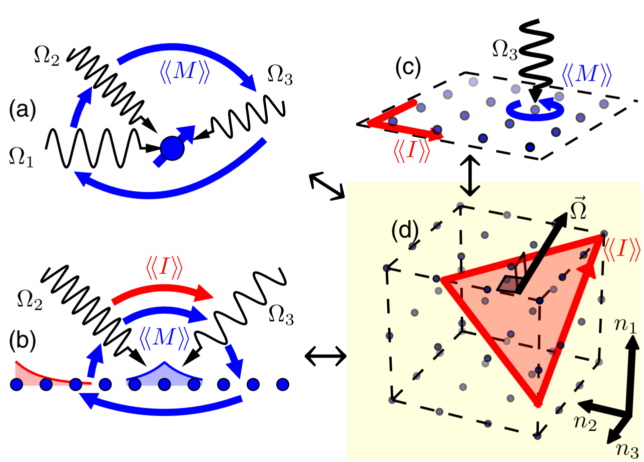


FIG. 1. Correspondence between ALTPs with fixed $d+D=3$. (a) $(0+3)$: A qudit driven by three incommensurate frequencies showing chiral circulation of energy $\langle\langle M\rangle\rangle$ between the drives. (b) $(1+2)$: A localized fermionic chain driven by two tones also exhibits an energy-charge circulation in the bulk and topological edge states that pump energy between the drives $\langle\langle I\rangle\rangle$. (c) $(2+1)$: A localized two-dimensional system driven by one tone has a quantized bulk magnetization and quantized edge currents [13,14]. (d) $(3+0)$: All three systems have a unifying description in terms of a static frequency lattice with localized bulk eigenstates and an electric field $\vec{\Omega}$.

 

The effects of quasiperiodic driving have been extensively studied in few-body systems [15–29] and more recently in many-body settings [30–37]. A cohesive frequency lattice lens allows us to significantly expand the number of dynamical phases accessible by quasiperiodic driving.

*Localization and the frequency lattice.*—Tight-binding models in $d$ spatial dimensions driven by $D$ incommensurate periodic tones are described by a Hamiltonian $H[\theta_{d+1}(t),\ldots,\theta_{d+D}(t)]$ (we use the indices $j\in\{1,\ldots,d\}$ for spatial dimensions). We assume $H$ is smooth and periodic in each of the $D$ drive phases $\theta_j(t)=\Omega_j t+\theta_{0j}$, where $\Omega_{d+i}$ is the angular frequency of the $i$th drive and $\theta_{0(d+i)}$ is its initial phase. For brevity of notation, we assemble the drive phases and frequencies into a vector such as $\vec{\Omega}=\sum_{j=d+1}^{d+D}\Omega_j\hat{e}_j$. The quasiperiodicity of the driving is stated formally as $H(\vec{\theta}_t)=H(\vec{\theta}_t+2\pi\hat{e}_j)$ [38].

We look for a basis of solutions to the Schrödinger equation of the form

$$|\psi_\alpha(t)\rangle=e^{-i\epsilon_\alpha t}|\phi_\alpha(\vec{\theta}_t)\rangle, \tag{1}$$

where $\alpha$ indexes the system's Hilbert space, $\epsilon_\alpha$ is a constant quasienergy, and $|\phi_\alpha(\vec{\theta})\rangle$ is a smooth quasienergy state defined on the torus of drive phases. Equation (1) is the generalization of the Floquet-Bloch decomposition to quasiperiodic driving [15,19,39]. Substituting Eq. (1) into the time-dependent Schrödinger equation, $i\partial_t|\psi_\alpha(t)\rangle=H(\vec{\theta}_t)|\psi_\alpha(t)\rangle$ (with $\hbar=1$), and Fourier transforming gives

$$\epsilon_\alpha|\phi_{\alpha\vec{n}}\rangle=\sum_{\vec{m}\in\mathbb{Z}^D}(H_{\vec{n}-\vec{m}}-\vec{n}\cdot\vec{\Omega}\delta_{\vec{n}\,\vec{m}})|\phi_{\alpha\vec{m}}\rangle, \tag{2}$$

where $H_{\vec{n}}$ and $|\phi_{\alpha\vec{n}}\rangle$ are the Fourier components of $H(\vec{\theta})$ and $|\phi_\alpha(\vec{\theta})\rangle$, respectively.

Introducing auxiliary degrees of freedom associated to the Fourier components $|\vec{n}\rangle$—a *frequency lattice*—allows the quasienergy states to be explicitly represented as the eigenstates $\sum_{\vec{n}\in\mathbb{Z}^D}|\phi_{\alpha\vec{n}}\rangle|\vec{n}\rangle$ of a quasienergy operator [15,19,40]:

$$K=\sum_{\vec{n},\vec{m}\in\mathbb{Z}^D}(H_{\vec{n}-\vec{m}}-\vec{n}\cdot\vec{\Omega}\delta_{\vec{n}\,\vec{m}})|\vec{n}\rangle\langle\vec{m}|. \tag{3}$$

$K$ has the form of a lattice Hamiltonian with an electric field $\vec{\Omega}$ and translationally invariant hopping matrices $H_{\vec{n}}$. As the $H_{\vec{n}}$ themselves act on a $d$-dimensional lattice, the full dimension of the frequency lattice is $d+D$, with $d$ spatial and $D$ synthetic dimensions. The frequency lattice is illustrated in Fig. 1(d) for $d+D=3$.

Although Eq. (3) holds for classical driving, it is useful to interpret the auxiliary state $|n_j\rangle$ as corresponding to the photon number of the $j$th drive [11]. A nearest-neighbor hop along direction $j$ then corresponds to photon emission or absorption into drive $j$, while the potential energy $\Omega_j n_j$ accounts for the energy of the drive.

We demand localization of the quasienergy states in the spatial dimensions for the purposes of stability of our classification. Localization ensures that small perturbations by local operators do not strongly couple distant quasienergy states, preventing the dramatic rearrangement of eigenstates that could otherwise occur.

Localization in the synthetic dimensions is then equivalent to the existence of a complete set of solutions (1). To see this, note that the Fourier expansion of the solution

$$|\psi_\alpha(t)\rangle=e^{-i\epsilon_\alpha t}|\phi_\alpha(\vec{\theta}_t)\rangle=e^{-i\epsilon_\alpha t}\sum_{\vec{n}\in\mathbb{Z}^D}|\phi_{\alpha\vec{n}}\rangle e^{-i\vec{n}\cdot\vec{\theta}_t} \tag{4}$$

converges only when the Fourier components $|\phi_{\alpha\vec{n}}\rangle$ are square summable, that is, when the eigenstates of $K$ are normalizable. When we have localization in both spatial and synthetic dimensions, we refer to the system as being in a localized phase.

An immediate dynamical consequence of localization is the quasiperiodic time dependence of local observables. This follows from the decomposition of an observable $O(t)$ in the Heisenberg picture in the basis of quasienergy states,

$$O(t)=\sum_{\alpha,\beta}O_{\alpha\beta}(\vec{\theta}_t)e^{-i(\epsilon_\beta-\epsilon_\alpha)t}|\phi_\alpha(\vec{\theta}_0)\rangle\langle\phi_\beta(\vec{\theta}_0)|, \tag{5}$$

where $O_{\alpha\beta}(\vec{\theta}_t)=\langle\phi_\alpha(\vec{\theta}_t)|O(0)|\phi_\beta(\vec{\theta}_t)\rangle$ is quasiperiodic. (We have assumed $O$ does not have explicit time dependence.) Roughly, localization of $|\phi_\alpha(\vec{\theta}_t)\rangle$ implies that only finitely many of the terms $O_{\alpha\beta}(\vec{\theta}_t)$ contribute significantly to expectation values, so that $\langle O(t)\rangle$ is explicitly quasiperiodic. Mathematically, the power spectrum of all local observables in a localized phase is pure point [18,19].

*Formal classification.*—The topological classification is most naturally expressed through the micromotion operator (cf. [41])

$$V(\vec{\Phi},\vec{\theta})=\sum_\alpha|\phi_\alpha(\vec{\theta})\rangle\langle\alpha|, \tag{6}$$

where $|\alpha\rangle$ is a basis for the system's Hilbert space and we have suppressed the dependence of the quasienergy states on the $d$ fluxes $\vec{\Phi}$ twisting the periodic boundary conditions of the spatial dimensions. In a localized phase the micromotion $V(\vec{\Phi},\vec{\theta})$ is a smooth map from the $(d+D)$-dimensional torus defined by $\vec{\Phi}$ and the drive phases $\vec{\theta}$ to the unitary group. It is well known that such maps are classified by an integer winding number $W[V]$ when $d+D$ is odd, defined by [42–45]

$$W[V]=C_{d+D}\int d^d\Phi d^D\theta\epsilon^{j\cdots k}\mathrm{Tr}[(V^\dagger\partial_j V)\cdots(V^\dagger\partial_k V)], \tag{7}$$

where the integral is over the torus, $\epsilon^{j\cdots k}$ is the Levi-Civita symbol, $\partial_j$ is differentiation with respect to one of $\Phi_j$ or $\theta_j$, and $C_{d+D}$ is a constant [46].

*Theorem.*—The winding number $W[V]$ is an integer valued topological invariant characterizing localized phases with $d+D>1$. That is, if the two Hamiltonian-frequency pairs $[H_0(\vec{\theta}), \vec{\Omega}_0]$ and $[H_1(\vec{\theta}), \vec{\Omega}_1]$ are joined by a connected path $[H_s(\vec{\theta}), \vec{\Omega}_s]$ (where $s \in [0,1]$) such that all the $[H_s(\vec{\theta}), \vec{\Omega}_s]$ have localized quasienergy states, then $W[V_0] = W[V_1]$.

In the Supplemental Material [46] we show that, under the conditions of the theorem, the path between the micromotion operators $V_s$ is continuous [53]. As $W[V]$ is invariant under smooth deformations of $V$ [42], the theorem follows [46]. We refer to a localized phase with a nontrivial winding number $W[V] \neq 0$ as an anomalous localized topological phase (ALTP).

As promised, the classification depends only on the frequency lattice dimension $d+D$. Note that the Floquet classification of anomalous phases without symmetry is reproduced with $D=1$ [41].

*Observable consequences.*—The formal classification of ALTPs is physically interesting only because it predicts quantized observables. The physical observables depend on $d$. We identify these for $d \in \{0,1\}$ when $d+D=3$ and later verify our predictions numerically (Fig. 2). The Floquet case $d=2$ is well studied [13,14].

The chiral energy circulation captures the topological response of $(0+3)$-dimensional ALTPs—qudits driven by three incommensurate tones. In more detail, the Heisenberg operator for the instantaneous rate of work done on the qudit is $U^\dagger \partial_t H(\vec{\theta}_t) U = \sum_j \Omega_j U^\dagger \partial_j H(\vec{\theta}_t) U$, where $U = U(t,0)$ is the evolution operator from time 0 to $t$. As energy input into the qudit must come from the drives, it is natural to identify $U^\dagger \partial_j H U \equiv -\dot{n}_j$ as the rate of photon transfer out of the $j$th drive. An operator measuring the rate at which photons circulate between the drives [Fig. 1(a)] is then

$$M(t) = \frac{1}{4}(\vec{n} \times \dot{\vec{n}}) \cdot \hat{\Omega} + \text{H.c.}, \tag{8}$$

where $\vec{n}$ is the integral of $\dot{\vec{n}}$, and we can drop the constant of integration [46]. Introducing the notation $\langle\langle A \rangle\rangle_T \equiv (1/T)\int_0^T dt \mathrm{Tr}[A(t)]$, we prove [46]

$$\langle\langle M \rangle\rangle_T = \frac{|\vec{\Omega}|}{2\pi} W[V] + O(T^{-1}). \tag{9}$$

That is, the long-time average of the circulation in an initial mixed state $\rho \propto \mathbb{1}$ is quantized and proportional to the winding number.

A quantized circulation is also present in $(1+2)$-dimensional ALTPs—wires driven by two incommensurate tones. However, in contrast to the $(0+3)$-dimensional ALTP, there are also *edge* signatures of topology.

At a boundary of the wire there is a topological *energy current* between the drives [Fig. 1(b)]. The frequency lattice for the driven wire has a slab geometry. A nonzero winding number in the bulk is accompanied by current-carrying edge states, which must run perpendicular to $\vec{\Omega}$, due to Stark localization by the electric field $\vec{\Omega}$ [Fig. 1(d)]. If $\vec{\Omega} = \Omega_2 \hat{e}_2 + \Omega_3 \hat{e}_3$, the edge current is parallel to $\Omega_3 \hat{e}_2 - \Omega_2 \hat{e}_3$. That is, photons are transferred from drive 3 to drive 2 (or drive 2 to drive 3, depending on the sign of $W[V]$) in an energy current.

Quantitatively, the long-time average of the energy current into drive $j$, $I_j(t) = \Omega_j \dot{n}_j(t)$, in an initial state localized near an edge is [46]

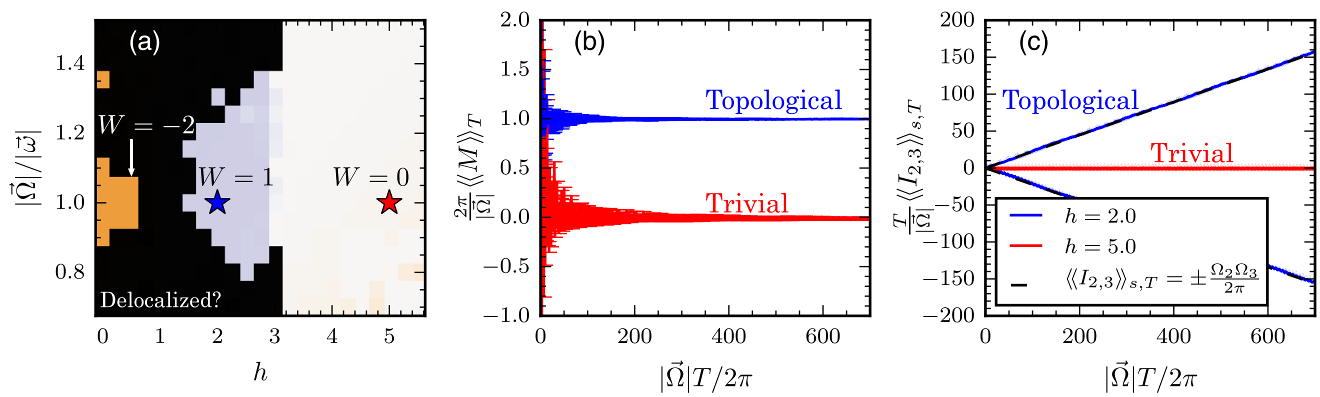


FIG. 2. Numerics for the model $H^\delta$. (a) $(0+3)$: Phase diagram. Colors represent the value of $\langle\langle M \rangle\rangle_T$ over a fixed time $T$. In black delocalized regions, the Fourier spectrum of $\langle\langle M \rangle\rangle_T$ is not pure point on numerical timescales. (b) $(0+3)$: $\langle\langle M \rangle\rangle_T$ for parameter values which are marked by stars in (a) against averaging time $T$. The average circulations converge to the theoretically predicted quantized values. (c) $(1+2)$: The work done on drive $j$ at one edge of the wire, $T\langle\langle I_j \rangle\rangle_{s,T}$ (10). Energy is transported between drives 2 and 3 at the predicted quantized average rate. Parameters: (a) $\delta/B_0 = 0.01$, $\vec{\omega}/B_0 = (2, 1.618031\ldots, 1.073506\ldots)$ and $\vec{\Omega} \propto \vec{\omega}$. (b) $\vec{\Omega} = \vec{\omega}$, $h=2$ (blue), and $h=5$ (red). (c) Lattice size $L=40$, $s=14$ sites filled; see Eq. (14). Further details are reported in [46].

$$\langle\langle I_j \rangle\rangle_{s,T} \equiv \langle\langle I_j \rho_s \rangle\rangle_T = \pm \frac{\Omega_2 \Omega_3}{2\pi} W[V] + O(T^{-1}, e^{-s/\xi}). \tag{10}$$

Here, $\rho_s$ is a projector onto lattice sites localized within $s$ sites of the edge, $\xi$ is the single-particle localization length, and the sign depends on which drive $j$ is being considered. Experimentally, this is the response of a noninteracting wire filled with fermions up to a distance $s$ from the edge.

*Model.*—Constructing a $(0+3)$-dimensional ALTP is difficult because simultaneously achieving localization in all the (synthetic) frequency lattice dimensions and a nonzero winding number is delicate. The electric field $\vec{\Omega}$ must be the cause of localization, as in the absence of $\vec{\Omega}$ the quasienergy operator $K$ is translationally invariant and all eigenstates are delocalized Bloch states. Indeed, a strong $\vec{\Omega}$ compared to the typical hopping amplitude $J$ does localize the quasienergy states, as adjacent sites in the frequency lattice become far detuned from one another. However, too short a localization length cannot lead to a nonzero circulation (9). By adding further-neighbor hops, we engineer a "sweet spot" with localization across a few sites and quantized circulation.

We construct a family of driven qubit models indexed by $\delta \geq 0$. We define $H^{\delta=0}(\vec{\theta}) = -(\vec{B}_1 + \vec{B}_2) \cdot \vec{\sigma}/2$, where $\vec{\sigma}$ is the vector of Pauli matrices, $\vec{B}_1$ corresponds to a short-range model on the frequency lattice, and $\vec{B}_2$ has the further-neighbor hops. Explicitly, $\vec{B}_1 = B_0 \langle \eta | \vec{\sigma} | \eta \rangle$, where

$$|\eta(\vec{\theta})\rangle = (\sin\theta_1 + i \sin\theta_2)|\uparrow\rangle + \left[\sin\theta_3 + i\left(h + \sum_{k=1}^{3} \cos\theta_k\right)\right]|\downarrow\rangle \tag{11}$$

is an unnormalized eigenstate of $\vec{B}_1 \cdot \vec{\sigma}$, and $h$ is a dimensionless parameter [54,55]. The field $\vec{B}_2$ is given by

$$\vec{B}_2 = \frac{[(\vec{\omega} \cdot \nabla)\vec{B}_1] \times \vec{B}_1}{|\vec{B}_1|^2}. \tag{12}$$

When the vector of parameters $\vec{\omega} = \vec{\Omega}$, this term acts as a counterdiabatic correction ensuring that the quasienergy states are parallel to $|\eta(\vec{\theta})\rangle$ [56,57]. Our choice of $|\eta(\vec{\theta})\rangle$ then allows for nonzero $W[V]$, depending on the value of $h$ [54,55]. For general $\delta > 0$ we truncate the Fourier spectrum of $H^{\delta=0}(\vec{\theta})$:

$$H^{\delta}(\vec{\theta}) = \sum_{\{\vec{n} : \|H^0_{\vec{n}}\|_F \geq \delta\}} e^{-i\vec{n}\cdot\vec{\theta}} H^0_{\vec{n}}, \tag{13}$$

where $H^0_{\vec{n}}$ are the Fourier coefficients of $H^{\delta=0}(\vec{\theta})$ and $\|\cdot\|_F$ is the Frobenius norm.

Figure 2(a) shows the phase diagram obtained by numerically solving the Schrödinger equation for $H^{\delta>0}$ with fifth-nearest-neighbor hops [58]. Three topological phases of winding numbers $W \in \{0, 1, -2\}$ are visible. The quantized energy circulation of these phases (9) is verified in Fig. 2(b).

The winding numbers coincide with those predicted by having quasienergy states parallel to $|\eta(\vec{\theta})\rangle$ near $\vec{\Omega} = \vec{\omega}$. For large enough frequency $|\vec{\Omega}| \gg B_0, |\vec{\omega}|$ the localization length is short and $W = 0$ (not shown). At lower frequencies $|\vec{\Omega}| \lesssim B_0$, $|\vec{\omega}|$ the quasienergy states may delocalize.

By reinterpreting one of the synthetic dimensions of $H^{\delta}(\vec{\theta})$ as spatial we obtain a $(1+2)$-dimensional model with ALTPs. Then the electric field causes localization in the spatial dimension. Explicitly, drive 1 (say) is replaced with a lattice of sites $|n_1\rangle$ with an electric potential $-\Omega_1 n_1$ and quasiperiodically time-dependent $m$-site hops:

$$H^{\delta}_m(\theta_2, \theta_3) = \int \frac{d\theta_1}{2\pi} e^{im\theta_1} H^{\delta}(\vec{\theta}). \tag{14}$$

Truncating the lattice provides the necessary edges to observe topological boundary effects.

Figure 2(c) confirms that the energy current is quantized (10). The exponential localization of the current-carrying modes at the edge can be observed in Fig. 3.

*Experimental prospects.*—$(0+D)$-dimensional ALTPs—driven qudits—are within immediate experimental reach in a number of solid-state and optical architectures [59–61]. Signatures of topology in the adiabatic limit have already been observed with two-tone-driven nitrogen vacancy centers [10].

$(1+2)$-dimensional ALTPs could be achieved in driven fermionic wires [5], but equivalent single-particle physics are available in several platforms [59,62–66], in particular, a qubit coupled to a quantum cavity [67] or a bosonic chain. In the former the "edge" at which an energy current occurs

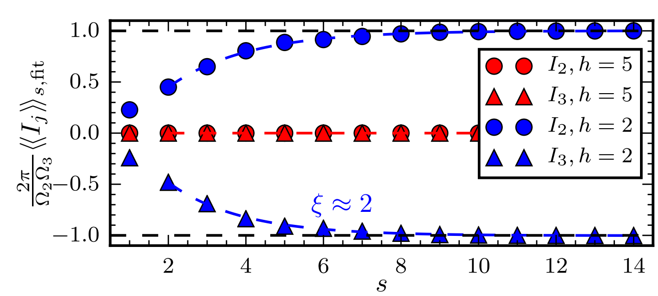


FIG. 3. Localization of edge modes. A fit to the slope of $T\langle\langle I_j \rangle\rangle_{s,T}$ with $T$ gives an estimate of the average current, $\langle\langle I_j \rangle\rangle_{s,\mathrm{fit}}$. The current increases exponentially toward the predicted value (10) as the number of initially filled sites $s$ is increased. An exponential fit in the topological regime gives a localization length of $\xi \approx 2$. Parameters: as in Fig. 2(c). Further details are reported in [46].

is the vacuum state. We demonstrate topological signatures in the qubit-cavity ALTP in [46].

An energy current between two drives can form the basis of many useful devices, e.g., conversion of photons from one frequency to another [7–9,32,34], cooling cavities [11], one-way circulation of energy between cavities, and the preparation of exotic cavity states [11,68]. The nonadiabatic energy currents of the $(1+2)$-ALTPs promise to make these devices faster and more stable.

*Outlook.*—We have derived a stable topological classification of quasiperiodically driven lattice models and identified the quantized observables that distinguish each phase. Localization in a dual frequency lattice is central to our understanding of these phases.

In one dimension, localization is believed to be stable to the addition of weak interactions [69–72]. We speculate that $d = 1$ ALTPs are stable interacting phases, even at infinite temperature, due to this many-body localization (MBL); see Refs. [73,74] for the $(2+1)$ case. The MBL ALTPs would provide new examples of localization-protected quantum order [75]. The bulk l bits of the MBL chain would support an energy-charge circulation, while the edge l bits would support energy currents.

We have discussed observable signatures for each ALTP with $d + D = 3$. A natural extension is determining the corresponding observables for larger numbers of drives and other symmetry classes. This would provide experimental access to the topological physics of driven systems in four dimensions and higher. To date, such responses have been observed only in the adiabatic limit [76,77].

The authors are grateful to I. Martin and C. Laumann for several helpful discussions. We would also like to thank E. Boyers, D. Else, M. Kolodrubetz, Y. Peng, M. Rudner, and A. Sushkov. Numerics were performed on the BU Shared Computing Cluster. This research was supported by NSF Grant No. DMR-1752759 and AFOSR Grant No. FA9550-20-1-0235.

*Note added.*—Recently, Ref. [78] appeared, which provides complementary models of $(1+2)$- and $(0+3)$-dimensional ALTPs. Where Ref. [78] overlaps with this work, they agree.

[*]dmlong@bu.edu


[1] D. J. Thouless, Phys. Rev. B **27**, 6083 (1983).
[2] M. Switkes, Science **283**, 1905 (1999).
[3] Y. E. Kraus, Y. Lahini, Z. Ringel, M. Verbin, and O. Zilberberg, Phys. Rev. Lett. **109**, 106402 (2012).
[4] M. Lohse, C. Schweizer, O. Zilberberg, M. Aidelsburger, and I. Bloch, Nat. Phys. **12**, 350 (2016).
[5] S. Nakajima, T. Tomita, S. Taie, T. Ichinose, H. Ozawa, L. Wang, M. Troyer, and Y. Takahashi, Nat. Phys. **12**, 296 (2016).
[6] P. Marra and M. Nitta, Phys. Rev. Research **2**, 042035(R) (2020).
[7] I. Martin, G. Refael, and B. Halperin, Phys. Rev. X **7**, 041008 (2017).
[8] P. J. D. Crowley, I. Martin, and A. Chandran, Phys. Rev. B **99**, 064306 (2019).
[9] P. J. D. Crowley, I. Martin, and A. Chandran, Phys. Rev. Lett. **125**, 100601 (2020).
[10] E. Boyers, P. J. D. Crowley, A. Chandran, and A. O. Sushkov, Phys. Rev. Lett. **125**, 160505 (2020).
[11] F. Nathan, I. Martin, and G. Refael, Phys. Rev. B **99**, 094311 (2019).
[12] F. Nathan, G. Refael, M. S. Rudner, and I. Martin, Phys. Rev. Research **2**, 043411 (2020).
[13] P. Titum, E. Berg, M. S. Rudner, G. Refael, and N. H. Lindner, Phys. Rev. X **6**, 021013 (2016).
[14] F. Nathan, M. S. Rudner, N. H. Lindner, E. Berg, and G. Refael, Phys. Rev. Lett. **119**, 186801 (2017).
[15] T.-S. Ho, S.-I. Chu, and J. V. Tietz, Chem, Phys. Lett. **96**, 464 (1983).
[16] J. Luck, H. Orland, and U. Smilansky, J. Stat. Phys. **53**, 551 (1988).
[17] G. Casati, I. Guarneri, and D. L. Shepelyansky, Phys. Rev. Lett. **62**, 345 (1989).
[18] H. R. Jauslin and J. L. Lebowitz, Chaos **1**, 114 (1991).
[19] P. M. Blekher, H. R. Jauslin, and J. L. Lebowitz, J. Stat. Phys. **68**, 271 (1992).
[20] À. Jorba and C. Simó, J. Differ. Equations **98**, 111 (1992).
[21] U. Feudel, A. S. Pikovsky, and M. A. Zaks, Phys. Rev. E **51**, 1762 (1995).
[22] D. Bambusi and S. Graffi, Commun. Math. Phys. **219**, 465 (2001).
[23] G. Gentile, Commun. Math. Phys. **242**, 221 (2003).
[24] S. I. Chu and D. A. Telnov, Phys. Rep. **390**, 1 (2004).
[25] R. Gommers, S. Denisov, and F. Renzoni, Phys. Rev. Lett. **96**, 240604 (2006).
[26] J. Chabé, G. Lemarié, B. Grémaud, D. Delande, P. Szriftgiser, and J. C. Garreau, Phys. Rev. Lett. **101**, 255702 (2008).
[27] D. Cubero and F. Renzoni, Phys. Rev. E **97**, 062139 (2018).
[28] S. Nandy, A. Sen, and D. Sen, Phys. Rev. B **98**, 245144 (2018).
[29] S. Ray, S. Sinha, and D. Sen, Phys. Rev. E **100**, 052129 (2019).
[30] S. Nandy, A. Sen, and D. Sen, Phys. Rev. X **7**, 031034 (2017).
[31] P. T. Dumitrescu, R. Vasseur, and A. C. Potter, Phys. Rev. Lett. **120**, 070602 (2018).
[32] M. H. Kolodrubetz, F. Nathan, S. Gazit, T. Morimoto, and J. E. Moore, Phys. Rev. Lett. **120**, 150601 (2018).
[33] Y. Peng and G. Refael, Phys. Rev. B **98**, 220509(R) (2018).
[34] Y. Peng and G. Refael, Phys. Rev. B **97**, 134303 (2018).
[35] H. Zhao, F. Mintert, and J. Knolle, Phys. Rev. B **100**, 134302 (2019).
[36] D. V. Else, W. W. Ho, and P. T. Dumitrescu, Phys. Rev. X **10**, 021032 (2020).
[37] A. J. Friedman, B. Ware, R. Vasseur, and A. C. Potter, arXiv:2009.03314.
[38] Throughout the main text we set $\vec{\theta}_0 = 0$, which is equivalent to shifting the origin of time for observables.
[39] G. Floquet, Ann. Sci. Ec. Norm. Super. **12**, 47 (1883).

[40] A. Verdeny, J. Puig, and F. Mintert, Z. Naturforsch., A: J. Phys. Sci. **71**, 897 (2016).
[41] R. Roy and F. Harper, Phys. Rev. B **96**, 155118 (2017).
[42] M. Nakahara, *Geometry, Topology and Physics*, 2nd ed. (IOP Publishing, Philadelphia, 2003).
[43] J. C. Y. Teo and C. L. Kane, Phys. Rev. B **82**, 115120 (2010).
[44] T. Kitagawa, E. Berg, M. Rudner, and E. Demler, Phys. Rev. B **82**, 235114 (2010).
[45] S. Yao, Z. Yan, and Z. Wang, Phys. Rev. B **96**, 195303 (2017).
[46] See Supplemental Material at http://link.aps.org/supplemental/10.1103/PhysRevLett.126.106805 for further details, which includes Refs. [47–52].
[47] M. S. Rudner, N. H. Lindner, E. Berg, and M. Levin, Phys. Rev. X **3**, 031005 (2013).
[48] F. Nathan and M. S. Rudner, New J. Phys. **17**, 125014 (2015).
[49] A. Eckardt and E. Anisimovas, New J. Phys. **17**, 093039 (2015).
[50] A. Kitaev, AIP Conf. Proc. **1134**, 22 (2009).
[51] T. Kato, *Perturbation Theory for Linear Operators*, 2nd ed. (Springer-Verlag, Berlin Heidelberg, 1980).
[52] N. Wiebe, D. Berry, P. Høyer, and B. C. Sanders, J. Phys. A **43**, 065203 (2010).
[53] In the $(0+1)$-dimensional case of a periodically driven qudit, $W[V]$ is not a good invariant, as it changes with a gauge transformation of the quasienergy states [46]. This case is peripheral to our focus on quasiperiodically driven systems.
[54] D.-L. Deng, S.-T. Wang, C. Shen, and L.-M. Duan, Phys. Rev. B **88**, 201105(R) (2013).
[55] F. N. Ünal, A. Eckardt, and R.-J. Slager, Phys. Rev. Research **1**, 022003(R) (2019).
[56] D. Sels and A. Polkovnikov, Proc. Natl. Acad. Sci. U.S.A. **114**, E3909 (2017).
[57] D. Guéry-Odelin, A. Ruschhaupt, A. Kiely, E. Torrontegui, S. Martínez-Garaot, and J. G. Muga, Rev. Mod. Phys. **91**, 045001 (2019).
[58] The $H^{\delta}$ used in our numerics has exponentially decaying hops up to fifth-nearest neighbor in the maximum norm, or eighth-nearest-neighbor in the 1-norm.
[59] M. Kjaergaard, M. E. Schwartz, J. Braumüller, P. Krantz, J. I.-J. Wang, S. Gustavsson, and W. D. Oliver, Annu. Rev. Condens. Matter Phys. **11**, 369 (2020).
[60] D. Leibfried, R. Blatt, C. Monroe, and D. Wineland, Rev. Mod. Phys. **75**, 281 (2003).
[61] M. W. Doherty, N. B. Manson, P. Delaney, F. Jelezko, J. Wrachtrup, and L. C. Hollenberg, Phys. Rep. **528**, 1 (2013).
[62] I. Bloch, J. Dalibard, and W. Zwerger, Rev. Mod. Phys. **80**, 885 (2008).
[63] L.-M. Duan and C. Monroe, Rev. Mod. Phys. **82**, 1209 (2010).
[64] P. Roushan *et al.*, Science **358**, 1175 (2017).
[65] T. Ozawa, H. M. Price, A. Amo, N. Goldman, M. Hafezi, L. Lu, M. C. Rechtsman, D. Schuster, J. Simon, O. Zilberberg, and I. Carusotto, Rev. Mod. Phys. **91**, 015006 (2019).
[66] J. D. Maynard, Rev. Mod. Phys. **73**, 401 (2001).
[67] T. Ozawa and H. M. Price, Nat. Rev. Phys. **1**, 349 (2019).
[68] D. M. Long, P. J. D. Crowley, and A. Chandran (unpublished).
[69] P. W. Anderson, Phys. Rev. **109**, 1492 (1958).
[70] D. M. Basko, I. L. Aleiner, and B. L. Altshuler, Ann. Phys. (Amsterdam) **321**, 1126 (2006).
[71] V. Oganesyan and D. A. Huse, Phys. Rev. B **75**, 155111 (2007).
[72] D. A. Abanin, E. Altman, I. Bloch, and M. Serbyn, Rev. Mod. Phys. **91**, 021001 (2019).
[73] F. Nathan, D. Abanin, E. Berg, N. H. Lindner, and M. S. Rudner, Phys. Rev. B **99**, 195133 (2019).
[74] F. Nathan, D. A. Abanin, N. H. Lindner, E. Berg, and M. S. Rudner, arXiv:1907.12228.
[75] D. A. Huse, R. Nandkishore, V. Oganesyan, A. Pal, and S. L. Sondhi, Phys. Rev. B **88**, 014206 (2013).
[76] M. Lohse, C. Schweizer, H. M. Price, O. Zilberberg, and I. Bloch, Nature (London) **553**, 55 (2018).
[77] O. Zilberberg, S. Huang, J. Guglielmon, M. Wang, K. P. Chen, Y. E. Kraus, and M. C. Rechtsman, Nature (London) **553**, 59 (2018).
[78] F. Nathan, R. Ge, S. Gazit, M. S. Rudner, and M. Kolodrubetz, arXiv:2010.11485.